**Mechanical
Sciences**

Open Access

A structure design method for compliant parallel manipulators with actuation isolation

Guangbo Hao[1] and Xianwen Kong[2]

[1]School of Engineering, University College Cork, Cork, Ireland
[2]School of Engineering and Physical Sciences, Heriot-Watt University, Edinburgh, EH14 4AS, UK

Correspondence to: Guangbo Hao (g.hao@ucc.ie)

Abstract. Since precise linear actuators of a compliant parallel manipulator suffer from their inability to tolerate the transverse motion/load in the multi-axis motion, actuation isolation should be considered in the compliant manipulator design to eliminate the transverse motion at the point of actuation. This paper presents an effective design method for constructing compliant parallel manipulators with actuation isolation, by adding the same number of actuation legs as the number of the DOF (degree of freedom) of the original mechanism. The method is demonstrated by two design case studies, one of which is quantitatively studied by analytical modelling. The modelling results confirm possible inherent issues of the proposed structure design method such as increased primary stiffness, introduced extra parasitic motions and cross-axis coupling motions.

1 Introduction

Compliant/flexure parallel manipulators (CPMs) have experienced rapid development over the two past decades due to their merits of eliminated backlash, friction, wear and lubrication as well as a reduced number of parts, which are very suitable for applications in precision engineering (macro scale) and MEMS (micro scale) (Smith, 2003; Howell et al., 2013). When high-precision motion is required, contact linear actuators such as piezoelectric (PZT) (Yue et al., 2010) and voice coil (VC) (Hiemstra et al., 2012) are the options because of their excellent positioning performances. However, these linear actuators conventionally suffer from their inability to tolerate the transverse motions/loads in the multi-axis motion requirements. Therefore, actuation isolation that is defined as eliminating the transverse motion at the point of actuation (Awtar and Slocum, 2007) should be considered in the CPM design. In compliant mechanisms, completely eliminating the transverse motion and allowing the actuation point to perfectly move along the actuation direction is impossible due to the nature of elasticity. Therefore, we aim to minimise the transverse motions of the linear actuator in the multi-axis motion system, by using a kind of decoupling mechanism that can transmit actuation force with negligible motion loss and can accommodate/absorb transverse motions

without producing transverse loads to the actuator (Awtar and Slocum, 2007).

There are a few successful methods to design CPMs, which include constraint-based method (Hale, 1999), FACT (Hopkins and Culpepper, 2010), and screw-theory-based method (Su et al., 2009). Those approaches mainly focus on design compliant *parallel* mechanisms/modules without considering actuation isolation. It is noteworthy to mention that great advances have been made in the conceptual design (type synthesis or structure synthesis) of rigid-link parallel mechanisms (see Kong and Gosselin, 2007 for example) since late 1990. The conceptual design of CPMs is closely-related to that of rigid-link parallel mechanisms. Even though several CPMs with actuation isolation have been proposed (Awtar et al., 2012; Hopkins and McCalib, 2012), the approaches are limited to special-DOF/-DOC or complex to use by engineers. Here and throughout this paper DOF and DOC stand for degree of freedom and degree of constraint, respectively.

Based on the above advances, this paper aims to propose a general method for the conceptual design of CPMs with actuation isolation, which intends to complement the existing methods. The remainder of this paper is organised as follows. Section 2 presents a general conceptual design ap-

proach by adding actuation legs. Case studies using the proposed method to design two CPMs with actuation isolation are discussed in Sect. 3. Analytical modelling is implemented in Sect. 4 to show the quantitative characteristic analysis of one resulting CPM. Section 5 draws the conclusions.

2 Constraint-based design approach

The design approach for actuation isolation in this section is a constraint-based design method, which is based on the following rule of rigid-link or compliant parallel mechanisms (see Kong and Gosselin, 2007 for instance):
Design rule: the addition of any number of 6-DOF legs to an original n-DOF (mostly parallel) mechanism results in a parallel mechanism with the same number of DOF and more legs.

The detailed procedure to design a CPM with actuation isolation is given below:

1. Design an *n*-DOF compliant mechanism without actuation isolation as the original mechanism using existing methods such as those in Hale (1999), Hopkins and Culpepper (2010) and Su et al. (2009);

2. Design the same number of extra compliant legs as the number of DOF specified in Step 1, where each leg is a simple 6-DOF serial mechanism that consists of a 1-DOF translational (or prismatic) joint and a 5-DOF straight wire beam with its axis along with the direction of the translational joint.

3. Connect the wire beam in each extra leg to the motion stage of the original mechanism to comply with the following conditions for arranging each leg:

    a. the connection point between the wire beam in one extra leg and the motion stage should be able to be actuated by the linear actuator guided by the translational joint; and

    b. *n* added extra legs working together should be able to effectively control the *n*-DOF of the original compliant mechanism by actuating the translational joint in each extra leg. This condition is the same as the validity condition of a set of *n* actuated joints for an *n*-DOF rigid-link parallel mechanism (Kong and Gosselin, 2007).

4. Appropriately arrange the configuration according to specific requirements.

Note that the wire beam (or other alternative design) in each extra leg offers the decoupling of the transverse motions on the actuation (Awtar et al., 2012; Hopkins et al., 2012) where the actuator is guided by a translational joint. The length of the wire beam in each added leg can be adjusted for specific reasons such as reducing the number of the DOF of the

actuation leg; and the translational joint can have different forms even though with amplification or direction-changing mechanisms. The above constraint-based design method can be seen as an "actuation-leg addition" method, which can be used to design any-DOF CPMs that are dominated by the original compliant mechanisms.

3 3-DOF CPM design cases

This section designs two 3-DOF CPMs for demonstrating the proposed actuation leg addition method: one is the in-plane 3-DOF 2T1R (T: translational; R: rotational) CPM (Fig. 1), and the other is the out-of-plane 3-DOF 2T1R CPM (Fig. 2).

3.1 In-plane 3-DOF CPM with actuation isolation

The design of the in-plane 3-DOF CPM starts from designing an original in-plane 3-DOF compliant mechanism without considering actuation isolation (Fig. 1a). This original planar mechanism consists of 4 identical parallel wire beams with no intersection point (intersection at infinitely far position), which can be designed using the emerging method (Hopkins and Culpepper, 2010; Su et al., 2009). By adding three extra 6-DOF legs (Fig. 1b) where the guiding translational joint is a leaf-type parallelogram mechanism, an in-plane 3-DOF CPM with actuation isolation is obtained as shown in Fig. 1c. The FEA (finite element analysis) motion demonstrations are illustrated in Fig. 1d–f, which show three individual motions in the DOF directions.

3.2 Out-of-plane 3-DOF CPM with actuation isolation

Designing the out-of-plane 3-DOF CPM also starts from designing an original out-of-plane 3-DOF mechanism without taking actuation isolation into account (Fig. 2a). This original out-of-plane mechanism is a symmetrical design for better performances. It is composed of 6 identical parallel wire beams in the same plane with more than one intersection points, where the distance between any two intersection points are large enough. This original mechanism was reported in Hao (2016), which can actually be seen as a type of well-known 6-DOF Gough-Stewart platform at its planar actuation singularity position. By adding three extra 6-DOF legs (Fig. 1b), an out-of-plane 3-DOF CPM with actuation isolation is obtained as shown in Fig. 2b. The FEA motion demonstrations are illustrated in Fig. 2c and d.

4 Theoretical modelling and analysis

Although the proposed design method in Sect. 2 can effectively address the issue of actuation isolation, it may be only valid with certain tolerances, i.e., it may introduce other problems such as parasitic motions and amplified actuation stiffness. In order to quantitatively assess the performance characteristics of the resulting CPM with actuation isolation

(a) An original in-plane 3-DOF (2T1R) parallel mechanism

(b) A 6-DOF serial mechanism: an extra leg

(c) A planar 3-DOF compliant parallel manipulator with actuation isolation

(d) Translation along the Y-axis by controlling two actuators with same displacement

(e) Translation along the X-axis by controlling one actuator

(f) Rotation by controlling one actuator
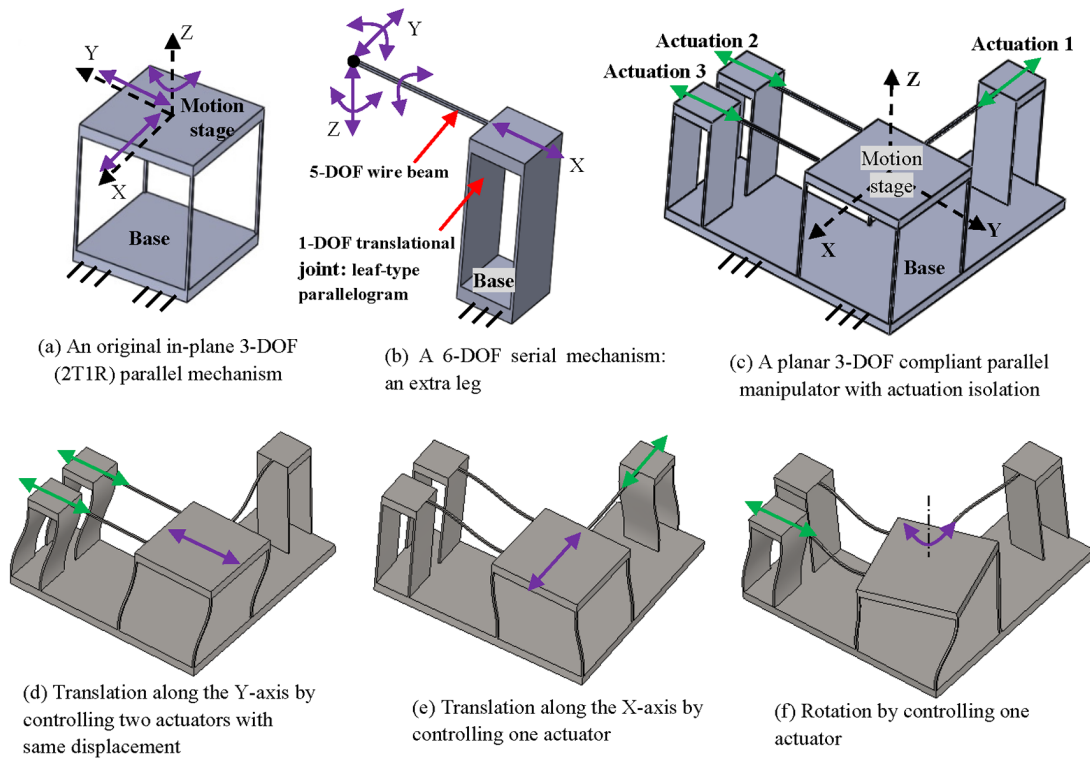
Figure 1. Design of an in-plane 3-DOF 2R1T CPM with actuation isolation.

(a) Original out-of-plane 3-DOF (2R1T) parallel mechanism

(c) FEA rotational result of the motion stage (with colour) by one actuation only

(b) 2R1T positioning stage

(d) FEA translational result of the motion stage by three equal actuations
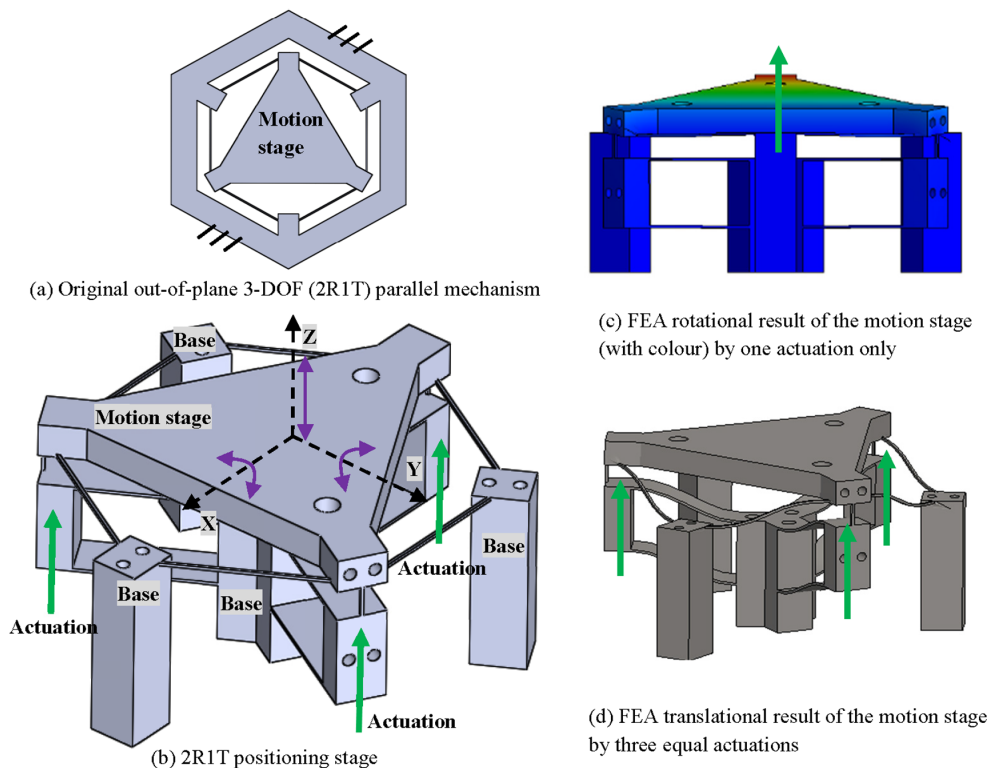
Figure 2. Design of an out-of-plane 3-DOF 2R1T CPM with actuation isolation.

(a) 6-DOF leg   (b) Top view of 3-DOF CPM   (c) Original mechanism
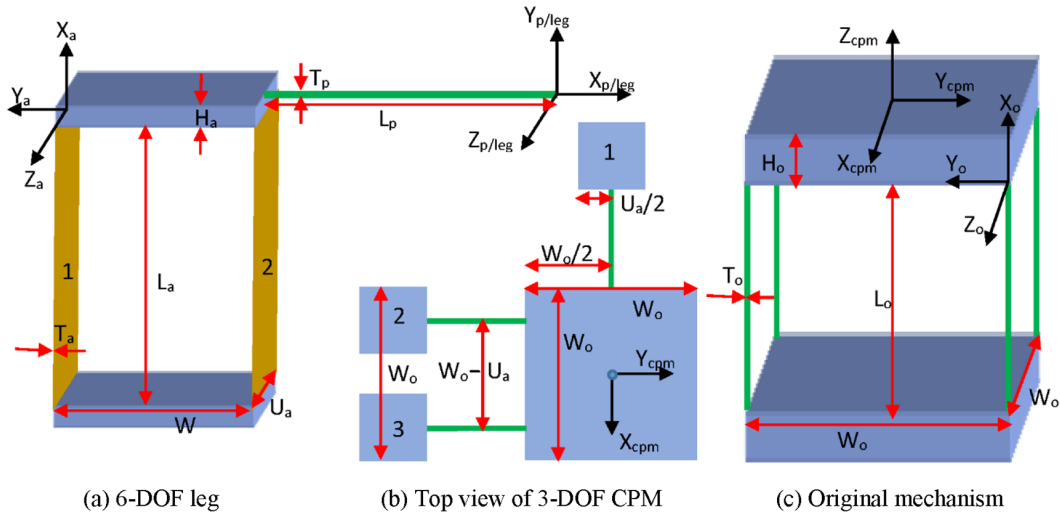
Figure 3. Geometry and coordinate system representations.

compared to its original mechanism, analytical modelling and compliance analysis with regard to the output motion stage can be carried out (Hao, 2016; Hao and Kong, 2013). It should be clarified that the motion range consideration of the modelled example based on the strength theory is out of scope of this paper.

We take the design in Fig. 1 with a specific legs' arrangement as an example for comprehensive analysis in this section, whose all geometry and coordinate system representations are clearly detailed in Fig. 3. All beams are assumed to have the same Young's modules (E) and the shear modulus (G) with uniform cross sections. Three extra legs are also identical. For simplifying expressions, we normalise geometrical dimensions by the original mechanism's characteristic length L_o, and normalise the force by EI_o/L_o^2, and moment by EI_o/L_o. Here, $I_o = T_o^4/12$, which is the second moment of inertia of square cross-section areas of identical beams in the original mechanism.

The stiffness matrix for the original mechanism with regard to the centre of the motion stage is to be developed at first based on the work in Hao and Kong (2013). The stiffness matrix of each wire beam with square cross sections in Fig. 3c is expressed as

$$\mathbf{K}_{ob} = \begin{bmatrix} 12/(T_o/L_o)^2 & 0 & 0 & 0 & 0 & 0 \\ 0 & 12 & 0 & 0 & 0 & -6 \\ 0 & 0 & 12 & 0 & 6 & 0 \\ 0 & 0 & 0 & 1.69G/E & 0 & 0 \\ 0 & 0 & 6 & 0 & 4 & 0 \\ 0 & -6 & 0 & 0 & 0 & 4 \end{bmatrix} \quad (1)$$

where $\mathbf{K}_{ob}$ is with regard to the local coordinate system $X_{oi} Y_{oi} Z_{oi}$ located at the centre of the mobile end of a wire beam. All geometrical parameters are explained in Fig. 3c. The normalised torsional stiffness (fourth row and fourth column) is calculated by considering warping influence (ignoring warping constraint) of a square cross section, where the

torsional moment of inertia ($2.25T_o^4/16$) is no longer double of the second moment of inertia of a square cross section (i.e., not equal to polar moment of inertia, $2T_o^4/12$) (Hao, 2016; Chen and Bai, 2016).

The stiffness matrix of the original mechanism can be then derived based on the rule of parallel systems as follows (Hao and Kong, 2013):

$$\mathbf{K}_o = \sum_{i=1}^{4} (\mathbf{T}_{oi})^T \mathbf{K}_{ob} \mathbf{T}_{oi} \quad (2a)$$

where $\mathbf{K}_o$ is with regard to the global coordinate system $X_{cpm} Y_{cpm} Z_{cpm}$ located at the (top-surface) centre of the motion stage of the original mechanism. $\mathbf{T}_{oi}$ is the transformation matrix from the local coordinate system $X_{oi} Y_{oi} Z_{oi}$ at the mobile-end centre of a wire beam to the global coordinate system, which is elaborated below:

$$\mathbf{T}_{oi} = \begin{bmatrix} \cos(\beta_i) & 0 & \sin(\beta_i) & 0 & 0 & 0 \\ 0 & 1 & 0 & 0 & 0 & 0 \\ -\sin(\beta_i) & 0 & \cos(\beta_i) & 0 & 0 & 0 \\ 0 & 0 & 0 & \cos(\beta_i) & 0 & \sin(\beta_i) \\ 0 & 0 & 0 & 0 & 1 & 0 \\ 0 & 0 & 0 & -\sin(\beta_i) & 0 & \cos(\beta_i) \end{bmatrix}$$
$$\begin{bmatrix} \cos(\gamma_i) & -\sin(\gamma_i) & 0 & 0 & 0 & 0 \\ \sin(\gamma_i) & \cos(\gamma_i) & 0 & 0 & 0 & 0 \\ 0 & 0 & 1 & 0 & 0 & 0 \\ 0 & 0 & 0 & \cos(\gamma_i) & -\sin(\gamma_i) & 0 \\ 0 & 0 & 0 & \sin(\gamma_i) & \cos(\gamma_i) & 0 \\ 0 & 0 & 0 & 0 & 0 & 1 \end{bmatrix}$$
$$\begin{bmatrix} 1 & 0 & 0 & 0 & dz_i & -dy_i \\ 0 & 1 & 0 & -dz_i & 0 & dx_i \\ 0 & 0 & 1 & dy_i & -dx_i & 0 \\ 0 & 0 & 0 & 1 & 0 & 0 \\ 0 & 0 & 0 & 0 & 1 & 0 \\ 0 & 0 & 0 & 0 & 0 & 1 \end{bmatrix} . \quad (2b)$$

In $\mathbf{T}_{\mathrm{o}i}$, $\beta_i = \pi/2$, $\gamma_i = \pi$, $dz_i = -H_\mathrm{o}/L_\mathrm{o}$ ($i = 1, 2, 3,$ or 4); $dx_1 = 0.5W_\mathrm{o}/L_\mathrm{o}$, $dy_1 = -0.5W_\mathrm{o}/L_\mathrm{o}$; $dx_2 = 0.5W_\mathrm{o}/L_\mathrm{o}$, $dy_2 = 0.5W_\mathrm{o}/L_\mathrm{o}$; $dx_3 = -0.5W_\mathrm{o}/L_\mathrm{o}$, $dy_3 = 0.5W_\mathrm{o}/L_\mathrm{o}$; $dx_4 = -0.5W_\mathrm{o}/L_\mathrm{o}$, $dy_4 = -0.5W_\mathrm{o}/L_\mathrm{o}$.

The compliance matrix of the original mechanism can be produced as

$$\mathbf{C}_\mathrm{o} = (\mathbf{K}_\mathrm{o})^{-1}. \tag{3}$$

The stiffness matrix for the extra leg is modelled in the following steps. Similar to Eq. (1), the 5-DOF wire beam with square cross sections in the extra leg (Fig. 3a) has its stiffness matrix with regard to its local coordinate system $X_\mathrm{p} Y_\mathrm{p} Z_\mathrm{p}$:

$$\mathbf{K}_{\mathrm{pb}} = \begin{bmatrix} \frac{T_\mathrm{p}^2}{L_\mathrm{p}}/\frac{I_\mathrm{o}}{L_\mathrm{o}^3} & 0 & 0 & 0 & 0 & 0 \\ 0 & 12\frac{I_\mathrm{p}}{L_\mathrm{p}^3}/\frac{I_\mathrm{o}}{L_\mathrm{o}^3} & 0 & 0 & 0 & -6\frac{I_\mathrm{p}}{L_\mathrm{p}^2}/\frac{I_\mathrm{o}}{L_\mathrm{o}^2} \\ 0 & 0 & 12\frac{I_\mathrm{p}}{L_\mathrm{p}^3}/\frac{I_\mathrm{o}}{L_\mathrm{o}^3} & 0 & 6\frac{I_\mathrm{p}}{L_\mathrm{p}^2}/\frac{I_\mathrm{o}}{L_\mathrm{o}^2} & 0 \\ 0 & 0 & 0 & 1.69\frac{GI_\mathrm{p}}{L_\mathrm{p}}/\frac{EI_\mathrm{o}}{L_\mathrm{o}} & 0 & 0 \\ 0 & 0 & 6\frac{I_\mathrm{p}}{L_\mathrm{p}^2}/\frac{I_\mathrm{o}}{L_\mathrm{o}^2} & 0 & 4\frac{I_\mathrm{p}}{L_\mathrm{p}}/\frac{I_\mathrm{o}}{L_\mathrm{o}} & 0 \\ 0 & -6\frac{I_\mathrm{p}}{L_\mathrm{p}^2}/\frac{I_\mathrm{o}}{L_\mathrm{o}^2} & 0 & 0 & 0 & 4\frac{I_\mathrm{p}}{L_\mathrm{p}}/\frac{I_\mathrm{o}}{L_\mathrm{o}} \end{bmatrix} \tag{4}$$

where $I_\mathrm{p} = T_\mathrm{p}^4/12$.

The stiffness matrix of a leaf beam in the 1-DOF translational joint can be obtained as below:

$$\mathbf{K}_{\mathrm{ab}} = \begin{bmatrix} \frac{T_\mathrm{a}^2}{L_\mathrm{a}}/\frac{I_\mathrm{o}}{L_\mathrm{o}^3} & 0 & 0 & 0 & 0 & 0 \\ 0 & 12\frac{I_{\mathrm{a}1}}{L_\mathrm{a}^3}/\frac{I_\mathrm{o}}{L_\mathrm{o}^3} & 0 & 0 & 0 & -6\frac{I_{\mathrm{a}1}}{L_\mathrm{a}^2}/\frac{I_\mathrm{o}}{L_\mathrm{o}^2} \\ 0 & 0 & 12\frac{I_{\mathrm{a}2}}{L_\mathrm{a}^3}/\frac{I_\mathrm{o}}{L_\mathrm{o}^3} & 0 & 6\frac{I_{\mathrm{a}2}}{L_\mathrm{a}^2}/\frac{I_\mathrm{o}}{L_\mathrm{o}^2} & 0 \\ 0 & 0 & 0 & \frac{GU_\mathrm{a}T_\mathrm{a}^3}{3L_\mathrm{a}}/\frac{EI_\mathrm{o}}{L_\mathrm{o}} & 0 & 0 \\ 0 & 0 & 6\frac{I_{\mathrm{a}2}}{L_\mathrm{a}^2}/\frac{I_\mathrm{o}}{L_\mathrm{o}^2} & 0 & 4\frac{I_{\mathrm{a}2}}{L_\mathrm{a}}/\frac{I_\mathrm{o}}{L_\mathrm{o}} & 0 \\ 0 & -6\frac{I_{\mathrm{a}1}}{L_\mathrm{a}^2}/\frac{I_\mathrm{o}}{L_\mathrm{o}^2} & 0 & 0 & 0 & 4\frac{I_{\mathrm{a}1}}{L_\mathrm{a}}/\frac{I_\mathrm{o}}{L_\mathrm{o}} \end{bmatrix} \tag{5}$$

where $\mathbf{K}_{\mathrm{ab}}$ is the matrix with regard to the local coordinate system $X_{\mathrm{a}i} Y_{\mathrm{a}i} Z_{\mathrm{a}i}$ located at the centre of the mobile end of a leaf beam. $I_{\mathrm{a}1} = U_\mathrm{a}T_\mathrm{a}^3/12$ and $I_{\mathrm{a}2} = T_\mathrm{a}U_\mathrm{a}^3/12$. The torsional stiffness for a rectangular cross section ($U_\mathrm{a} > 10T_\mathrm{a}$) is calculated by considering warping influence (ignoring warping constraint) (Hao and Kong, 2013; Chen and Bai, 2016).

The stiffness matrix of the translational joint composed of two identical leaf beams can be derived as follows (Hao, 2016):

$$\mathbf{K}_\mathrm{a} = \sum_{i=1}^{2} (\mathbf{T}_{\mathrm{a}i})^T \mathbf{K}_{\mathrm{ab}} \mathbf{T}_{\mathrm{a}i} \tag{6a}$$

where $\mathbf{K}_\mathrm{a}$ is derived with regard to the coordinate system $X_\mathrm{p} Y_\mathrm{p} Z_\mathrm{p}$. $\mathbf{T}_{\mathrm{a}i}$ is the transformation matrix from the local coordinate system $X_{\mathrm{a}i} Y_{\mathrm{a}i} Z_{\mathrm{a}i}$ at the mobile-end centre of a leaf beam to the coordinate system $X_\mathrm{p} Y_\mathrm{p} Z_\mathrm{p}$, which is detailed below:

$$\mathbf{T}_{\mathrm{a}i} = \begin{bmatrix} \cos(\gamma_i) & -\sin(\gamma_i) & 0 & 0 & 0 & 0 \\ \sin(\gamma_i) & \cos(\gamma_i) & 0 & 0 & 0 & 0 \\ 0 & 0 & 1 & 0 & 0 & 0 \\ 0 & 0 & 0 & \cos(\gamma_i) & -\sin(\gamma_i) & 0 \\ 0 & 0 & 0 & \sin(\gamma_i) & \cos(\gamma_i) & 0 \\ 0 & 0 & 0 & 0 & 0 & 1 \end{bmatrix}$$

$$\begin{bmatrix} 1 & 0 & 0 & 0 & dz_i & -dy_i \\ 0 & 1 & 0 & -dz_i & 0 & dx_i \\ 0 & 0 & 1 & dy_i & -dx_i & 0 \\ 0 & 0 & 0 & 1 & 0 & 0 \\ 0 & 0 & 0 & 0 & 1 & 0 \\ 0 & 0 & 0 & 0 & 0 & 1 \end{bmatrix}. \tag{6b}$$

In $\mathbf{T}_{\mathrm{a}i}$, $\gamma_i = -\pi/2$, $dz_i = 0$ ($i = 1$ or 2); $dx_1 = -(W_\mathrm{a} + L_\mathrm{p})/L_\mathrm{o}$, $dy_1 = -H_\mathrm{a}/L_\mathrm{o}$; $dx_2 = -L_\mathrm{p}/L_\mathrm{o}$, $dy_2 = -H_\mathrm{a}/L_\mathrm{o}$.

Therefore, the compliance matrix of the extra leg can be derived based on the rule of serial systems (Hao and Kong, 2013) as:

$$\mathbf{C}_{\mathrm{leg}} = (\mathbf{K}_\mathrm{a})^{-1} + (\mathbf{K}_{\mathrm{pb}})^{-1} \tag{7}$$

where the leg's compliance matrix $\mathbf{C}_{\mathrm{leg}}$ is based on the coordinate system $X_{\mathrm{leg}} Y_{\mathrm{leg}} Z_{\mathrm{leg}}$ overlapping with the local coordinate system $X_\mathrm{p} Y_\mathrm{p} Z_\mathrm{p}$.

Finally, the stiffness matrix, with regard to the global coordinate system $X_{\mathrm{cpm}} Y_{\mathrm{cpm}} Z_{\mathrm{cpm}}$, of the resulting CPM with actuation isolation is shown:

$$\mathbf{K}_{\mathrm{cpm}} = \sum_{i=1}^{3} (\mathbf{T}_{\mathrm{leg}i})^T (\mathbf{C}_{\mathrm{leg}})^{-1} \mathbf{T}_{\mathrm{leg}i} + \mathbf{K}_\mathrm{o} \tag{8a}$$

where $\mathbf{T}_{\mathrm{leg}i}$ is the transformation matrix from the leg's coordinate system $X_{\mathrm{leg}i} Y_{\mathrm{leg}i} Z_{\mathrm{leg}i}$ to the global coordinate system $X_{\mathrm{cpm}} Y_{\mathrm{cpm}} Z_{\mathrm{cpm}}$, which is explained below:

$$\mathbf{T}_{\mathrm{leg}i} = \begin{bmatrix} 1 & 0 & 0 & 0 & 0 & 0 \\ 0 & \cos(\alpha_i) & -\sin(\alpha_i) & 0 & 0 & 0 \\ 0 & \sin(\alpha_i) & \cos(\alpha_i) & 0 & 0 & 0 \\ 0 & 0 & 0 & 1 & 0 & 0 \\ 0 & 0 & 0 & 0 & \cos(\alpha_i) & -\sin(\alpha_i) \\ 0 & 0 & 0 & 0 & \sin(\alpha_i) & \cos(\alpha_i) \end{bmatrix}$$

$$\begin{bmatrix} \cos(\gamma_i) & -\sin(\gamma_i) & 0 & 0 & 0 & 0 \\ \sin(\gamma_i) & \cos(\gamma_i) & 0 & 0 & 0 & 0 \\ 0 & 0 & 1 & 0 & 0 & 0 \\ 0 & 0 & 0 & \cos(\gamma_i) & -\sin(\gamma_i) & 0 \\ 0 & 0 & 0 & \sin(\gamma_i) & \cos(\gamma_i) & 0 \\ 0 & 0 & 0 & 0 & 0 & 1 \end{bmatrix}$$

$$\begin{bmatrix} 1 & 0 & 0 & 0 & dz_i & -dy_i \\ 0 & 1 & 0 & -dz_i & 0 & dx_i \\ 0 & 0 & 1 & dy_i & -dx_i & 0 \\ 0 & 0 & 0 & 1 & 0 & 0 \\ 0 & 0 & 0 & 0 & 1 & 0 \\ 0 & 0 & 0 & 0 & 0 & 1 \end{bmatrix}. \tag{8b}$$

In $\mathbf{T}_{\mathrm{leg}i}$ ($i = 1, 2$ or 3): $\alpha_1 = \alpha_2 = \alpha_3 = -\pi/2$; $\gamma_1 = 0$, $\gamma_2 = \gamma_3 = -\pi/2$; $dx_1 = -0.5W_\mathrm{o}/L_\mathrm{o}$, $dx_2 = -0.5(W_\mathrm{o} - U_\mathrm{a})/L_\mathrm{o}$, $dx_3 = 0.5(W_\mathrm{o} - U_\mathrm{a})/L_\mathrm{o}$; $dy_1 = 0$, $dy_2 = -0.5W_\mathrm{o}/L_\mathrm{o}$, $dy_3 = -0.5W_\mathrm{o}/L_\mathrm{o}$; $dz_1 = dz_2 = dz_3 = [H_\mathrm{a} + L_\mathrm{a} - (H_\mathrm{o} + L_\mathrm{o})]/L_\mathrm{o}$.

The compliance matrix of the CPM with actuation isolation can be thus obtained as

$$\mathbf{C}_{\text{cpm}} = \left(\mathbf{K}_{\text{cpm}}\right)^{-1}. \tag{9}$$

Let $L_a = 50\,\text{mm}$, $T_a = 0.75\,\text{mm}$, $W_a = 12\,\text{mm}$, $H_a = 10\,\text{mm}$, $U_a = 12\,\text{mm}$; $T_p = 2\,\text{mm}$, $L_p = 50\,\text{mm}$; $T_o = 2\,\text{mm}$, $L_o = 50\,\text{mm}$, $W_o = 50\,\text{mm}$, $H_o = 10\,\text{mm}$; $E = 69\,000\,\text{MPa}$ and $G = 26\,000\,\text{MPa}$, the linear compliance matrices for the original mechanism and the CPM with actuation isolation, respectively, are shown below:

$$\mathbf{C}_o = \begin{bmatrix} 2.09 \times 10^{-2} & 0 & 0 & 0 & 9.33 \times 10^{-5} & 0 \\ 0 & 2.09 \times 10^{-2} & 0 & -9.33 \times 10^{-5} & 0 & 0 \\ 0 & 0 & 3.33 \times 10^{-5} & 0 & 0 & 0 \\ 0 & -9.33 \times 10^{-5} & 0 & 1.33 \times 10^{-4} & 0 & 0 \\ 9.33 \times 10^{-5} & 0 & 0 & 0 & 1.33 \times 10^{-4} & 0 \\ 0 & 0 & 0 & 0 & 0 & 3.77 \times 10^{-2} \end{bmatrix} \tag{10a}$$

$$\mathbf{C}_{\text{cpm}} = \begin{bmatrix} 1.47 \times 10^{-2} & -7.02 \times 10^{-4} & -4.53 \times 10^{-7} & 2.95 \times 10^{-6} & 6.38 \times 10^{-5} & -4.91 \times 10^{-3} \\ -7.02 \times 10^{-4} & 1.43 \times 10^{-2} & -9.49 \times 10^{-7} & -6.06 \times 10^{-5} & -2.94 \times 10^{-6} & 2.56 \times 10^{-3} \\ -4.53 \times 10^{-7} & -9.49 \times 10^{-7} & 3.33 \times 10^{-5} & 9.89 \times 10^{-8} & -4.95 \times 10^{-8} & -7.34 \times 10^{-9} \\ 2.95 \times 10^{-6} & -6.06 \times 10^{-5} & 9.89 \times 10^{-8} & 1.33 \times 10^{-4} & 1.22 \times 10^{-8} & -1.08 \times 10^{-5} \\ 6.38 \times 10^{-5} & -2.94 \times 10^{-6} & -4.95 \times 10^{-8} & 1.22 \times 10^{-8} & 1.33 \times 10^{-4} & -2.06 \times 10^{-5} \\ -4.91 \times 10^{-3} & 2.56 \times 10^{-3} & -7.34 \times 10^{-9} & -1.08 \times 10^{-5} & -2.06 \times 10^{-5} & 1.79 \times 10^{-2} \end{bmatrix}. \tag{10b}$$

Equations (10a) and (10b) both show the agreement that the diagonal compliance entries corresponding to the DOF directions (primary compliance) are comparable, and are at least 100 times larger than other compliance entries corresponding to the DOC directions. This means that the added extra legs does not change the mobility of the original mechanism.

However, in comparison with the original mechanism the added legs with the current specific arrangement can result in two problems as below, exposing trade-offs to be considered:

1. The extra legs do increase the stiffness in the DOF directions, which is reflected by the decreased primary compliances in Eq. (10b). For the analysis case study in this section, the primary compliances of the CPM with actuation isolation are reduced by 29.67 % in the x axis, by 31.58 % in the y axis, and by 52.52 % about the z axis, respectively. However, there is no observation on the compliance/stiffness change of the motion stage in the DOC directions since the DOC stiffness of the original mechanisms is much larger (100 times larger) than the added stiffness in the same directions.

2. The added legs can cause issues associated with parasitic motions (related to DOC) and cross-axis coupling (related to DOF) that do not exist in the original mechanism. For instance, the force, applied on the origin of the global coordinate system along the x axis, cannot only produce the primary translation along the x axis (primary compliance 1.47×10^{-2}), but also parasitic translation in the z axis (parasitic compliance -4.53×10^{-7}), parasitic rotation about the x axis (parasitic compliance 2.95×10^{-6}), and cross-axis coupling motions along the y axis (coupling compliance -7.02×10^{-4}) and about the z axis (coupling compliance -4.91×10^{-3}).

Note that the resulting CPM with actuation isolation has alleviated existing parasitic rotation in the y axis (or x axis)

caused by the force along the x axis (or y axis), with a reduction of 31.62 % (or 35.05 %). Observing Eq. (10b), we can see that if the compliance entries below the order of 10^{-4} can be neglected due to the accuracy tolerance, all parasitic motions vanish while only cross-axis coupling compliance terms remain.

The above analytical modelling method can also be used to quantitatively analyse the stiffness/compliance of the proposed out-of-plane 3-DOF CPM with actuation isolation (Fig. 2), which is left for the future work. The modelling results would be useful to identify if the added legs are able to actuate all DOF directions and/or if there exists decoupling between input and output. If each primary compliance in the compliance matrix of the resulting CPM includes the contribution of at least one of the actuation compliances of the translational joints in added legs, all DOF are actively controllable. It should be mentioned that a 6-DOF CPM with actuation isolation can be proposed using the method presented in Sect. 2 where the original compliant mechanism is a 0-DOC (6-DOF) mechanism (free rigid body). The 6-DOF CPM is composed of six actuation legs, each of which serially consists of a 1-DOF translational joint and a 5-DOF wire beam with its axis along with the direction of the translational joint. For practical reasons, the six wire beams are arranged in three pairs along three orthogonal directions (Hale, 1999).

5 Conclusions

An actuation-leg addition approach has been presented in this paper for the conceptual design of any-DOF CPMs with actuation isolation. The added leg is a 6-DOF serial chain, which is a very simple design in compliant mechanisms and can be arranged in different desired positions. This method provides an universal/general solution to consider actuation isolation for any (compliant) parallel mechanisms. Two design studies have been implemented with one case analytically modelled. The linear modelling results quantitatively show that the added extra legs, although obtaining the actuation isolation, may cause several inherent problems including increased primary stiffness, introduced extra parasitic motions and cross-axis coupling motions.

It is hoped that the proposed method can be used as an initial solution for further comprehensive modelling and geometrical optimization of CPMs towards specific applications. Trade-offs should be carefully considered between the strength and weakness using actuation isolation. Further experimental verification is also to be investigated.

The Supplement related to this article is available online at doi:10.5194/ms-7-247-2016-supplement.

References

Awtar, S. and Slocum, A. H.: Constraint-based design of parallel kinematic XY flexure mechanisms, ASME J. Mech. Design, 129, 816–830, 2007.

Awtar, S., Ustick, J., and Sen, S.: An XYZ parallel kinematic flexure mechanism with geometrically decoupled degrees of freedom, ASME J. Mech. Robot., 5, 015001, doi:10.1115/1.4007768, 2012.

Chen, G. and Bai, R.: Modeling Large Spatial Deflections of Slender Bisymmetric Beams in Compliant Mechanisms Using Chained Spatial-Beam Constraint Model, J. Mech. Robot., 8, 041011, doi:10.1115/1.4032632, 2016.

Hale, L. C.:Principles and Techniques for Designing Precision Machines, PhD thesis, Massachusetts Institute of Technology, Cambridge, MA, 1999.

Hao, G.: Determinate design and analytical analysis of a class of symmetrical flexure guiding mechanisms for linear actuators, J. Mech. Design, 139, 012301-1–012301-12, 2016.

Hao, G. and Kong, X.: A normalization-based approach to the mobility analysis of spatial compliant multi-beam modules, Mech. Mach. Theory, 59, 1–19, 2013.

Hiemstra, D. B., Parmar, G., and Awtar, S.: Performance tradeoffs posed by moving magnet actuators in flexure-based nanopositioning, ASME/IEEE T. Mechatron., 99, 1–12, 2012.

Hopkins, J. B. and Culpepper, M. L.:, Synthesis of multi-degree of freedom, parallel flexure system concepts via freedom and constraint topology (FACT) – Part I: Principles, Precis. Eng., 34, 259–270, 2010.

Hopkins, J. B. and McCalib, D. B.: Synthesizing precision flexures that decouple displacement-based actuators, in: 27th Annual Meeting of the American Society for Precision Engineering, 21–26 October 2012, San Diego, CA, 2012.

Howell, L. L., Magleby, S. P., and Olsen, B. M.: Handbook of Compliant Mechanisms, Wiley, New York, 2013.

Kong, X. and Gosselin, M.: Type Synthesis of Parallel Mechanisms, Springer-Verlag, Berlin, 2007.

Smith, S. T.: Flexures: Elements of Elastic Mechanisms, Taylor and Francis, London, 2003.

Su, H. J., Denis, V. D., and Judy, M. V.: A screw theory approach for the conceptual design of flexible joints for compliant mechanisms, ASME J. Mech. ' Robot., 1, 041009, doi:10.1115/1.3211024, 2009.

Yue, Y., Gao, F., Zhao, X., and Ge, Q.: Relationship among input-force, payload, stiffness and displacement of a 3-DOF perpendicular parallel micro-manipulator, Mech. Mach. Theory, 45, 756–771, 2010.